Dynamical pion production via parametric resonance from disoriented chiral condensates

Hideaki Hiro-Oka
Institute of Physics, Kitasato University, 1-15-1 Kitasato Sagamihara, Kanagawa 228-8555, Japan

Hisakazu Minakata
Department of Physics, Tokyo Metropolitan University, 1-1 Minami-Osawa, Hachioji, Tokyo 192-0397, Japan
and Research Center for Cosmic Neutrinos, Institute for Cosmic Ray Research, University of Tokyo, Tanashi, Tokyo 188-8502, Japan
(Received 8 June 1999; published 10 March 2000)

We discuss a dynamical mechanism of pion production from disoriented chiral condensates. It leads to an explosive production of pions via the parametric resonance mechanism, which is similar to the reheating mechanism in inflationary cosmology. Classically it is related with the instability in the solutions of the Mathieu equation and we explore the quantum aspects of the mechanism. We show that nonlinearities and back reactions can be ignorable for a sufficiently long time under the small amplitude approximations of background σ oscillations, which may be appropriate for the late stage of a nonequilibrium phase transition. It allows us to obtain an explicit quantum state of the produced pions and σ, the squeezed state of BCS type. Single particle distributions and two pion correlation functions are computed within these approximations. The results obtained illuminate the characteristic features of multipion states produced through the parametric amplification mechanism. In particular, two pion correlations of various charge combinations contain back-to-back correlations which cannot be masked by the identical particle interference effect. We suggest that the parametric resonance mechanism might be a cause of the long lasting amplification of low-momentum modes in linear sigma model simulations.

PACS number(s): 25.75.Gz, 11.10.Ef, 25.75.Dw

I. INTRODUCTION

We now believe in quantum chromodynamics (QCD) as *the* theory of strong interaction. Yet, the Centauro and anti-Centauro events that were found in cosmic ray experiments [1] indicate some puzzling features. The events are characterized by large fluctuations in the ratio of the number of neutral pions to that of charged pions. It appeared to be unlikely that such a feature can be realized inside the conventional picture of hadronic interactions with ''soft'' QCD interaction, which implies more or less an independent emission of particles.

However, several authors formulated a scenario which explains such features of the events based on the idea of formation of chirally misaligned domains, the disoriented chiral condensate (DCC) [2,3]. It requires that a ''hot'' matter forms during hadronic collisions in which the chiral symmetry is restored, and then rapidly cools down so that chiral orientation of the pion fields can align to a random direction different from that of the vacuum. If the low-momentum mode of the pion fields are enhanced large domains of definite (but random in direction) isospin would form. Then, a large isospin, and therefore charge fluctuations, naturally result.

The amplification of low-momentum pion modes was demonstrated by Rajagopal and Wilczek [4] by doing a numerical simulation of the linear sigma model using the quench initial condition. A more explicit confirmation of the formation of large domains was provided by Asakawa, Huang, and Wang [5] who computed pion-field correlation functions by using an elaborated simulation code which takes into account expansion along the longitudinal as well as the transverse direction.

One should note, however, that the large charge-neutral fluctuation does not necessarily imply a random isotropic (in isospin space) rolling down from the top of the Mexican hat potential. As was shown by Greiner, Gong, and Müller [6] any isosinglet multipion states approximately have the well-known neutral fraction distribution $P(f)$:

$$P(f)=\frac{1}{2\sqrt{f}}, \tag{1}$$

where

$$f=\frac{N_{\pi^0}}{N_{\pi^0}+N_{\pi^+}+N_{\pi^-}}. \tag{2}$$

We note that this distribution was in fact derived by only requiring the isospin singlet phase space [7]. Therefore the large charge-neutral fluctuation may merely imply an isospin singlet DCC state, not a random isotropic rolling down.

The interpretation of the results of the simulation by Rajagopal and Wilczek [4] also requires reexamination. They interpreted the origin of the amplification of the low-momentum pion mode as due to instability of the Nambu-Goldstone modes of chirally symmetric field configurations at around the top of the Mexican hat. However, the enhancement of the low-momentum pion modes actually take place with a much longer time scale than that of rolling down motion, $\sim 1/m_\sigma$, as one can clearly see in Fig. 1 in their paper. Then, we need to identify a certain mechanism which is responsible for the enhancement. The most likely candidate, in our opinion, is the parametric resonance mechanism [8,9]. The mechanism, possibly being tied up with a new instability that arises within the approximation scheme we

will take, seems to be capable of explaining qualitative features of long lasting amplification of low-momentum modes (see Secs. III and VI). Some other aspects of formation mechanism of DCC were explored in Refs. [10–13].

In a previous paper [15], we briefly explored the parametric resonance mechanism emphasizing its characteristic features in the two pion correlations, and its possible relevance as a hunting tool of DCC. In this paper we examine the mechanism in detail, hoping that it will shed some light on the origin of enhancement of the low-momentum pion modes. We focus on the pion production at around the bottom of the Mexican hat potential. It may be an appropriate setting at least for the late stage of nonequilibrium phase transition which would result in the formation of coherent DCC domains.

Furthermore, we concentrate on the case that the sigma model fields oscillate along the σ direction. In fact, it is shown in the numerical simulation [5] that sigma model field configurations rapidly point to the σ direction in a time scale of the order of $\sim 1/m_\pi$. Under the background oscillation of the σ field the quantum fluctuations of the pion and the σ fields can be excited. If the frequencies of background and quantum fluctuations match with each other the fluctuations are parametrically amplified, leading to an explosive pion production.

We emphasize that the mechanism of pion production from DCC which we explore in this paper differs from that usually adopted in the literature [2–4], as we mentioned earlier. In the conventional picture of pion emission from DCC, one assumes that the sigma model fields roll down along the direction (in most cases) different from the σ direction. Then, the field configurations relax toward the σ direction, the orientation of the QCD vacuum, which entails the coherent pion emission through the relaxation process. In contrast, pion production takes place even when the sigma model fields rolls down along the σ direction in our parametric resonance mechanism. To indicate this point, we propose in the next section a set of approximations that leads to a simplified but a concrete model field theory that allows us to construct explicitly the produced multipion quantum state.

We should remark that we do not claim that the parametric resonance is the whole story. Formation and decay of DCC is a complicated nonlinear phenomenon. The instability associated with the Nambu-Goldstone modes is an indispensable ingredient for triggering the growth of the low-momentum pion modes. But, we also stress that it is *not* enough either. In Sec. VI we will calculate the power spectrum of pion and sigma fields in our framework and attempt a qualitative comparison with the result obtained in Rajagopal-Wilczek's simulation. It will give us a feeling on the question of to what extent the amplification of power is due to the parametric resonance mechanism.

Even though the parametric resonance mechanism is the cause of the long lasting amplification of low-momentum modes we still lack understanding of how the initial instability is mediated to it [14]. Leaving understanding of this last point to future investigations, our emphasis in this paper is that if the parametric resonance mechanism is operative at the late stage of the nonequilibrium phase transition it may give clear signatures which should be useful for its experimental hunting.

In Sec. II, we introduce the linear sigma model, formulate the system with parametric resonance by introducing successive approximations in various stages, and make clear that to what extent the approximations are valid. In Sec. III, we quantize the system in a conventional way of quantizing a system of quantum fields, and clarify the relationship with the other formulation. In Sec. IV, we calculate the single particle distributions of pions and σ to demonstrate a characteristic feature of the parametric resonance mechanism. In Sec. V we discuss the two pion correlations which display another characteristic feature of the mechanism. We argue that they can be used as powerful experimental hunting tool of DCC. In Sec. VI we compute the power spectrum of pion and sigma fields and examine the qualitative features of the amplification of power in our framework. In the last section we will summarize our investigation, give concluding remarks, and discuss the limitations of our framework. In Appendix A, we summarize the feature of multiparticle states implied by the single mode squeezed state. In Appendix B, we derive sum rule obeyed by isospin invariance and the isosinglet nature of the multiparticle state within the framework of single mode treatment.

II. MODEL AND APPROXIMATIONS

The Lagrangian of the linear sigma model is given by

$$\mathcal{L}=\frac{1}{2}\partial_\mu\phi_a\partial^\mu\phi_a-\frac{\lambda}{4}(\phi_a\phi_a-v_0^2)^2+h\sigma, \tag{3}$$

where $\phi_a=(\sigma,\vec{\pi})$. The typical values of the parameters which are relevant for phenomenology of QCD are

$$\lambda=20, \quad v_0=90 \text{ MeV}, \quad m_\pi=\sqrt{\frac{h}{v_0}}=140 \text{ MeV}. \tag{4}$$

These values of the parameters will be used in the numerical analysis in later sections.

As discussed in the previous section we deal with the pion production that takes place when the sigma model fields are at around the bottom of the Mexican hat potential, which may be realized in the time scale of $\sim 1/m_\pi$ after rolling down. We assume that at this stage the sigma model fields oscillate along the σ direction. For clarity we construct a further simplified model by doing successive approximations in the linear sigma model that allow us to explicitly construct the produced multipion quantum state.

We expand the sigma model fields at around the minimum of the Mexican hat potential along the σ direction:

$$\begin{aligned}\chi&=\sigma-v,\\ \vec{\pi}&=\vec{\pi}.\end{aligned} \tag{5}$$

The linear sigma model Lagrangian, then, takes the form

$$\mathcal{L}[\chi,\vec{\pi}]=\frac{1}{2}(\partial_\mu\chi)^2-\frac{\lambda}{2}(3v^2-v_0^2)\chi^2-\lambda v\chi^3-\frac{\lambda}{4}\chi^4 + \frac{1}{2}(\partial_\mu\vec{\pi})^2-\frac{1}{2}m_\pi^2\vec{\pi}^2-\lambda v\chi\vec{\pi}^2-\frac{1}{2}\lambda\chi^2\vec{\pi}^2 - \frac{1}{4}\lambda\vec{\pi}^4. \tag{6}$$

Following Mrówczyński and Müller [9], we make a further approximation of decomposing σ model fields into the classical time-dependent background fields and the quantum fluctuations around them:

$$\chi(\boldsymbol{x},t)=\chi_0(t)+\eta(\boldsymbol{x},t), \qquad \vec{\pi}(\boldsymbol{x},t)=\vec{\pi}_0(t)+\vec{\xi}(\boldsymbol{x},t). \tag{7}$$

We have assumed the spatial homogeneity of the background fields. It may be a reasonable assumption if we work inside a single domain because the key feature of DCC is its coherence over a domain. Of course, it is a simplifying assumption in a real physical situation, but is an inevitable one in order to make the treatment technically manageable. Substituting Eq. (7) into Lagrangian (6), we have

$$\mathcal{L}[\chi_0+\eta,\vec{\pi}_0+\vec{\xi}]=\mathcal{L}[\chi_0,\vec{\pi}_0]+\frac{1}{2}(\partial\eta)^2-\frac{1}{2}[m_\sigma^2 + 3\Sigma(t)]\eta^2-\frac{1}{2}\lambda\vec{\pi}_0^2\eta^2-\lambda(\chi_0+v)\eta^3 - \frac{1}{4}\lambda\eta^4+\frac{1}{2}(\partial\vec{\xi})^2-\frac{1}{2}[m_\pi^2+\Sigma(t)]\vec{\xi}^2 - \frac{3}{2}\lambda\vec{\pi}_0^2\vec{\xi}^2-\lambda\vec{\pi}_0\vec{\xi}^3-\frac{1}{4}\lambda\vec{\xi}^4-2\lambda v\vec{\pi}_0\eta\vec{\xi} - \lambda(\chi_0+v)\eta\vec{\xi}^2-\lambda\vec{\pi}_0\vec{\xi}\eta^2-\frac{1}{2}\lambda\eta^2\vec{\xi}^2, \tag{8}$$

where $m_\sigma=\sqrt{\lambda(3v^2-v_0^2)}$ and v is the minimum value of the σ direction determined by the equation $\lambda(\sigma^2-v_0^2)\sigma-h=0$. For small h, v is given approximately by $v=v_0+h/2\lambda v^2$. Due to the background field oscillation, a time-dependent term $\Sigma(t)$ arises in the mass terms of $\vec{\xi}$ and η fluctuations and is given by $\Sigma=\lambda\chi_0(\chi_0+2v)$. The terms linearly proportional to fluctuations, of course, vanish due to the equations of motion of the background fields:

$$\ddot{\chi}_0+\lambda\chi_0^3+3\lambda v\chi_0^2+m_\sigma^2\chi_0+\lambda(\chi_0+v)\vec{\pi}_0^2=0, \tag{9}$$

$$\ddot{\vec{\pi}}_0+m_\pi^2\vec{\pi}_0+2\lambda v\chi_0\vec{\pi}_0+\lambda\chi_0^2\vec{\pi}_0+\lambda\vec{\pi}_0^3=0. \tag{10}$$

We work with the ansatz that the background fields oscillate along the σ direction, and set $\vec{\pi}_0=0$ in the subsequent analyses. We further restrict ourselves into the regime, $|\chi_0/v|\ll 1$, in which the nonlinear terms in χ_0's equation of motion are negligible. Then, the solution to the χ_0's equation of motion takes the harmonic form

$$\chi_0(t)=\tilde{\chi}_0\cos(m_\sigma t+\varphi), \tag{11}$$

where φ is an initial phase which we set to vanish for simplicity. In the numerical analysis performed in Sec. IV, we will use $|\chi_0/v|=0.05$ ($\times$ 1/2, 1, 2) for illustrative purposes.

We should note that the limitation of small amplitude oscillation that we have imposed, $|\chi_0/v|\ll 1$, restricts the validity of our treatment only to a qualitative level. Nevertheless, we believe that it is a meaningful starting point, and in fact it makes theoretical analysis transparent as we will see below.

We differ from Mrówczyński and Müller [9] by treating η and $\vec{\xi}$ quantum mechanically. The equations of motion obeyed by fluctuations η and $\vec{\xi}$ are given as

$$\partial^2\eta+m_\sigma^2\eta+3(2\lambda v\chi_0+\lambda\chi_0^2)\eta+2\lambda(\chi_0+v)\eta^2+\lambda\eta^3=0, \tag{12}$$

$$\partial^2\vec{\xi}+m_\pi^2\vec{\xi}+(2\lambda v\chi_0+\lambda\chi_0^2)\vec{\xi}+\lambda\vec{\xi}^3=0.$$

They are greatly simplified by the restriction of small oscillation amplitudes of background fields.

Let us first focus on the pion fluctuations. The χ_0^2 term is ignorable compared to $v\chi_0$ term because of the restriction of $|\chi_0/v|\ll 1$. The $v\chi_0$ term is also small compared with the mass term, but we shall keep it otherwise we lose the parametric resonance. The cubic term of $\vec{\xi}$ is negligible until the time scale

$$z\sim\frac{m_\sigma^2}{4\lambda v\tilde{\chi}_0}\ln\left(\frac{(m_\sigma/2)^2-2\lambda v\tilde{\chi}_0}{10\lambda}\right), \tag{13}$$

where the dimensionless time z is measured by m_σ as $2z=m_\sigma t+\varphi+\pi$. For instance, it can be numerically estimated as $z\sim 67$ for $|\chi_0/v|=0.05$.

We have ignored the quantum back reactions to the pionic and sigma fluctuations due to particle production. It could be taken into account, e.g., by the Hartree-Fock approximation. Instead of going through this treatment, we estimate the time scale until which it can be negligible. It is given roughly as

$$z\sim\frac{m_\sigma^2}{4\lambda v\tilde{\chi}_0}\ln\left(\frac{m_\sigma^2\tilde{\chi}_0}{10\lambda(\tilde{\chi}_0+v)}\right), \tag{14}$$

and the same numerical examination indicates that it is at $z\sim 32$.

We emphasize therefore that under the approximation of small amplitude oscillation of background fields, ignoring nonlinear terms in the field fluctuations is a good approximation in a fairly long time even for such strong coupling as $\lambda=20$.

We end up with the equation of motion of sigma and pionic fluctuations:

$$\left[\frac{d^2}{dz^2}+A_\sigma-2q_\sigma\cos(2z)\right]\eta_{\boldsymbol{k}}(z)=0, \tag{15}$$

$$\left[\frac{d^2}{dz^2}+A_\pi-2q_\pi\cos(2z)\right]\vec{\xi}_{\boldsymbol{k}}(z)=0, \tag{16}$$

where

$$A_\sigma\equiv\frac{4(\boldsymbol{k}^2+m_\sigma^2)}{m_\sigma^2},\quad q_\pi\equiv\frac{12\lambda v\tilde{\chi}_0}{m_\sigma^2}, \tag{17}$$

and

$$A_\pi\equiv\frac{4(\boldsymbol{k}^2+m_\pi^2)}{m_\sigma^2},\quad q_\pi\equiv\frac{4\lambda v\tilde{\chi}_0}{m_\sigma^2}, \tag{18}$$

$\eta_{\boldsymbol{k}}$ and $\vec{\xi}_{\boldsymbol{k}}$ denote the Fourier components of the fields $\eta_{\boldsymbol{x}}$ and $\vec{\xi}(\boldsymbol{x})$, respectively. Equations (15) and (16) are known as the Mathieu equation and are known to admit unstable solutions for a wide range of parameters of A's and q's. See, e.g., Ref. [16]. Such an unstable solution may be interpreted as explosive particle production under the background of oscillating χ_0 fields.

III. QUANTUM EVOLUTION OF SYSTEM AND SQUEEZED STATE

We discuss in this section the quantum evolution of the time-dependent states of $\vec{\pi}$ and σ fluctuations. Thanks to the restrictions and approximations introduced in the previous section, the structure of quantum states formed by η and $\vec{\xi}$ quanta can be analyzed analytically.

We start by writing the Hamiltonian in a form analogous to the harmonic oscillators but with time-dependent frequencies:

$$H=\int d^3k\left[\frac{1}{2}P_{\boldsymbol{k}}P_{-\boldsymbol{k}}+\frac{1}{2}\Omega_{\boldsymbol{k}}^\sigma(t)^2Q_{\boldsymbol{k}}Q_{-\boldsymbol{k}}\right]+\sum_j\int d^3k\left[\frac{1}{2}P_{\boldsymbol{k}}^jP_{-\boldsymbol{k}}^j+\frac{1}{2}\Omega_{\boldsymbol{k}}^\pi(t)^2Q_{\boldsymbol{k}}^jQ_{-\boldsymbol{k}}^j\right], \tag{19}$$

where

$$\Omega_{\boldsymbol{k}}^\sigma(t)^2=\boldsymbol{k}^2+m_\sigma^2+6\lambda v\chi_0(t),$$
$$\Omega_{\boldsymbol{k}}^\pi(t)^2=\boldsymbol{k}^2+m_\pi^2+2\lambda v\chi_0(t). \tag{20}$$

The variables $Q_{\boldsymbol{k}}$ and $Q_{\boldsymbol{k}}^j$ in Eq. (19) are defined by

$$\eta(\boldsymbol{x},t)=\int\frac{d^3k}{(2\pi)^3}e^{i\boldsymbol{k}\cdot\boldsymbol{x}}Q_{\boldsymbol{k}}(t),\ \xi^j(\boldsymbol{x},t)=\int\frac{d^3k}{(2\pi)^3}e^{i\boldsymbol{k}\cdot\boldsymbol{x}}Q_{\boldsymbol{k}}^j(t), \tag{21}$$

and $P_{\boldsymbol{k}}$ and $P_{\boldsymbol{k}}^j$ are, as usual, the conjugate momenta of $Q_{\boldsymbol{k}}$ and $Q_{\boldsymbol{k}}^j$, respectively. The index j runs over 1 to 3, and we take the adjoint representation for the isotriplet pion fields. For its concrete form, we refer Appendix B. One can see that the equations of motion (15) and (16) are derived from this Hamiltonian.

Within the small background oscillation we can take that $(\chi_0/v)<(m_\pi/m_\sigma)^2$. This restriction guarantees that the frequency $\Omega_{\boldsymbol{k}=0}^\pi$ is real, which is necessary in our present treatment which ignores quantum back reactions. If the background oscillation amplitude is larger than the critical value the system has an instability which we referred to as a new instability in the Introduction. It definitely arises within our approximation and is indicative of a remnant of the Rajagopal-Wilczek instability because it arises only for negative χ_0 (which means toward central maximum of the Mexican hat). Nevertheless, the new instability has a characteristic feature that is quite different from that of the Rajagopal-Wilczek's. The former can continue for long time while the latter lasts only a time scale of $1/m_\sigma$. Notice that both of the instabilities that we are talking about are the local instabilities, not the real global ones which totally destabilize the whole system.

The nature of the instability, however, is not transparent to us. When one works with certain truncations in highly nonlinear systems one can easily generate instabilities which may or may not be possessed by the original system. There are instabilities whose origin one can easily understand from simple consideration. For example, pion fields can have local instability by generating the winding motion encircling around the bottom of a wine bottle when the field energy of background σ field oscillation with amplitude χ_0 exceeds the symmetry breaking energy, that is, $\frac{1}{2}m_\sigma^2\chi_0^2>m_\pi^2v^2$. It leads to the condition for onset of the instability $\chi_0/v>m_\pi/m_\sigma$.

But the instability we encountered above occurs at a much smaller amplitude, $(\chi_0/v)>(m_\pi/m_\sigma)^2$. To our knowledge, there is no intuitive way of understanding the instability. It can be the artifact of our approximation and truncation scheme and, if this is the case, may be cured by taking nonlinearities and back reactions into account.

In the rest of the paper we will restrict ourselves to the small amplitude regime of the background σ oscillation so that we are free from the new instability. In Sec. VII we will briefly discuss its role together with the parametric resonance as a possible candidate mechanism for understanding the long-lasting amplification of powers in sigma model simulations.

The quantum theory of harmonic oscillators with time-dependent frequencies was developed some time ago. In a previous paper [15] we followed the formalism developed by Shtanov, Traschen, and Brandenberger (STB) [17], but we shall present in this paper an equivalent but more conventional formalism of quantizing the same system. From the form of the Hamiltonian (19), we can discuss sigma and pion sectors collectively; we treat below the sigma sector but with suppressing the superscript σ, and it can be regarded as that of pion sector in which the superscript π as well as isospin index are suppressed.

We decompose the dynamical variables in momentum space in terms of solutions of the equations of motion

$$Q_{\boldsymbol{k}}(t)=Q_1(t)a_{0\boldsymbol{k}}+Q_2(t)a^{\dagger}_{0-\boldsymbol{k}},$$
$$P_{\boldsymbol{k}}(t)=\dot{Q}_1(t)a_{0-\boldsymbol{k}}+\dot{Q}_2(t)a^{\dagger}_{0\boldsymbol{k}}, \tag{22}$$

where Q_1 and Q_2 are the solutions to the equation of motion of Q derived from the Hamiltonian

$$\ddot{Q}_{\boldsymbol{k}}(t)+\Omega^2_{\boldsymbol{k}}(t)Q_{\boldsymbol{k}}(t)=0. \tag{23}$$

Notice that $Q_2=Q_1^*$. $a_{0\boldsymbol{k}}$ and $a^{\dagger}_{0\boldsymbol{k}}$ are the annihilation and the creation operators, respectively. They are time-independent, i.e., they obey the Heisenberg equation of motion as

$$\frac{da_{0\boldsymbol{k}}}{dt}\equiv\frac{\partial a_{0\boldsymbol{k}}}{\partial t}+i[H,a_{0\boldsymbol{k}}]=0. \tag{24}$$

The consistency condition between the commutation relations, i.e.,

$$[a_{0\boldsymbol{k}},\,a^{\dagger}_{0\boldsymbol{k}}]=1,\quad [Q_{\boldsymbol{k}},\,P_{\boldsymbol{k}'}]=i\,\delta(\boldsymbol{k}-\mathbf{k}'), \tag{25}$$

is achieved by the Wronskian condition

$$Q_1\dot{Q}_2-\dot{Q}_1Q_2=i. \tag{26}$$

Substituting Eq. (22) into Eq. (19), we obtain the following form:

$$H_{\boldsymbol{k}}=\int d^3k\ \frac{1}{2}[A_k a_{0\boldsymbol{k}}a_{0-\boldsymbol{k}}+A_k^* a^{\dagger}_{0\boldsymbol{k}}a^{\dagger}_{0-\boldsymbol{k}} +B_k(a^{\dagger}_{0\boldsymbol{k}}a_{0\boldsymbol{k}}+a_{0\boldsymbol{k}}a^{\dagger}_{0\boldsymbol{k}})], \tag{27}$$

where the coefficients $A_{\boldsymbol{k}}$ and $B_{\boldsymbol{k}}$ are defined by

$$A_{\boldsymbol{k}}=\dot{Q}_1^2+\Omega^2_{\boldsymbol{k}}Q_1^2,\quad B_{\boldsymbol{k}}=\dot{Q}_1\dot{Q}_2+\Omega^2_{\boldsymbol{k}}Q_1Q_2. \tag{28}$$

Note that $A_{\boldsymbol{k}}$ is complex number, and that Q_1 and Q_2 are complex conjugate with each other. On the other hand, $B_{\boldsymbol{k}}$ is real as far as $\Omega_{\boldsymbol{k}}$ is real, which is the case owing to our restriction to small background oscillations.

In order to diagonalize the Hamiltonian (27), we introduce the Bogoliubov transformation as

$$a_{0\boldsymbol{k}}(t)=\alpha^*_{\boldsymbol{k}}(t)a_{\boldsymbol{k}}-\beta^*_{\boldsymbol{k}}(t)a^{\dagger}_{-\boldsymbol{k}},$$
$$a^{\dagger}_{0\boldsymbol{k}}(t)=\alpha_{\boldsymbol{k}}(t)a^{\dagger}_{\boldsymbol{k}}-\beta_{\boldsymbol{k}}(t)a_{-\boldsymbol{k}}, \tag{29}$$

with

$$\alpha_{\boldsymbol{k}}(t)=e^{i\varphi_\alpha}\cosh\theta_{\boldsymbol{k}},\quad \beta_{\boldsymbol{k}}(t)=e^{i\varphi_\beta}\sinh\theta_{\boldsymbol{k}}. \tag{30}$$

Choosing θ_k as

$$\tanh 2\,\theta_{\boldsymbol{k}}=\frac{|A_{\boldsymbol{k}}|}{B_{\boldsymbol{k}}}, \tag{31}$$

one can diagonalize the Hamiltonian into the form

$$H_{\boldsymbol{k}}=\Omega_{\boldsymbol{k}}a^{\dagger}_{\boldsymbol{k}}(t)a_{\boldsymbol{k}}(t), \tag{32}$$

where use has been made of the Wronskian relation (26) to show that the coefficient of Eq. (32) is in fact given by $\Omega_{\boldsymbol{k}}$. Therefore the operator $a_{\boldsymbol{k}}(t)$ defined in Eq. (29) does represent annihilation operator of physical quanta at time t. Using Eq. (31) with Eq. (28) it is easy to show that

$$\cosh^2\theta_{\boldsymbol{k}}=\frac{B_{\boldsymbol{k}}+\Omega_{\boldsymbol{k}}}{2\Omega_{\boldsymbol{k}}},\quad \sinh^2\theta_{\boldsymbol{k}}=\frac{B_{\boldsymbol{k}}-\Omega_{\boldsymbol{k}}}{2\Omega_{\boldsymbol{k}}}. \tag{33}$$

In the above treatment, we have relied on the fact that amplitudes of the background oscillation is small so that $\Omega_{\boldsymbol{k}}$ is real. If we remove this assumption the system experiences instability in a certain period of time. It is not a totally unstable system due to the nature of the instability and it would be interesting to work out such a system. However, we do not engage in such business in the present paper. Instead, we argue that it is important to take account of back reactions in addressing such a problem. It could even be the case that the quantum back reaction entirely cures the instability.

Let us move on to the analysis of the eigenstates for the effective Hamiltonian. We define the vacua $|0\rangle$ and $|0(t)\rangle$ as

$$a_{0\boldsymbol{k}}|0\rangle=0,\quad a_{\boldsymbol{k}}(t)|0(t)\rangle=0, \tag{34}$$

and assume that the oscillator at $t=0$ is in the vacuum state $|0\rangle$, i.e., $|0(t=0)\rangle=|0\rangle$. It leads to the initial conditions for $\alpha_{\boldsymbol{k}}(t)$ and $\beta_{\boldsymbol{k}}(t)$:

$$|\alpha_{\boldsymbol{k}}(0)|=1,\quad \beta_{\boldsymbol{k}}(0)=0. \tag{35}$$

The physical quantum with momentum $\boldsymbol{k}$ is created (annihilated) by $a^{\dagger}_{\boldsymbol{k}}(t)$ $[a_{\boldsymbol{k}}(t)]$, because the Hamiltonian is diagonalized by them at each time t. As the system evolves, the state $|0\rangle$ is no longer the vacuum annihilated by $a_{\boldsymbol{k}}(t)$.

We rewrite the Bogoliubov transformation (29) into the form of unitary transformation:

$$a_{0\boldsymbol{k}}=e^{-i\varphi_\alpha}e^{-G_{\mathbf{k}}(t)}a_{\boldsymbol{k}}(t)e^{G_{\mathbf{k}}(t)},$$
$$a^{\dagger}_{0\boldsymbol{k}}=e^{i\varphi_\alpha}e^{-G_{\mathbf{k}}(t)}a^{\dagger}_{\boldsymbol{k}}(t)e^{G_{\mathbf{k}}(t)}, \tag{36}$$

where

$$G_{\mathbf{k}}(t)=\theta_{\mathbf{k}}(a^{\dagger}_{\mathbf{k}}a^{\dagger}_{-\mathbf{k}}-a_{\mathbf{k}}a_{-\mathbf{k}}). \tag{37}$$

From the definitions of vacua (34) and of transformation (36), we have

$$|0\rangle=e^{-G_k(t)}|0(t)\rangle. \tag{38}$$

After a short calculation [19], we obtain the vacuum state of the form

$$|0\rangle=\prod_{\boldsymbol{k}}\frac{1}{\sqrt{|\alpha_{\boldsymbol{k}}(t)|}}\exp\left[\frac{\beta^*_{\boldsymbol{k}}}{2\alpha^*_{\boldsymbol{k}}}a^{\dagger}_{\boldsymbol{k}}(t)a^{\dagger}_{-\boldsymbol{k}}(t)\right]|0(t)\rangle. \tag{39}$$

The state is known as the squeezed state and is widely used in quantum optics [18]. A significant feature of Eq. (39) is

that it has pairing correlation between back-to-back momentum configurations, namely $\boldsymbol{k}$ and $-\boldsymbol{k}$, modes, and we will refer to it as the squeezed state of BCS type in this paper. In the next two sections, we will discuss, in detail, the characteristic features of particle production due to the parametric resonance mechanism. Earlier discussions of the squeezed state in the context of DCC may be found in Refs. [19] and [20]. We also note that the particle production via the parametric resonance has been extensively discussed in the context of reheating in the inflationary universe [21–23], and a mechanism for producing superheavy dark matter [24].

Before closing this section, we would like to comment on the relationship between our formalism and the one by Shtanov, Traschen, and Brandenberger [17] which can provide a description of quantum systems with parametric resonances. Since we have adopted their formalism in our previous paper, we will try to compare and clarify the relation between various quantities that appear in both formalisms.

In short, there is a simple relationship between two formalisms: they start from the time-dependent operator [our $a_{\boldsymbol{k}}(t)$] which diagonalizes the Hamiltonian and then Bogoliubov transform it to the time-independent operator $a_{0\boldsymbol{k}}$. Therefore such a correspondence is likely to exist.

In order to make the correspondence more precise, we write down the equations obeyed by the coefficients of the Bogoliubov transformation in both formalisms. In STB formalism, they read

$$\dot{\alpha}_{\boldsymbol{k}}(t)=\frac{\dot{\Omega}_{\boldsymbol{k}}}{2\Omega_{\boldsymbol{k}}}\beta_{\boldsymbol{k}}\cdot e^{2i\int^t\Omega_{\boldsymbol{k}}dt'},$$
$$\dot{\beta}_{\boldsymbol{k}}(t)=\frac{\dot{\Omega}_{\boldsymbol{k}}}{2\Omega_{\boldsymbol{k}}}\alpha_{\boldsymbol{k}}\cdot e^{-2i\int^t\Omega_{\boldsymbol{k}}dt'}. \tag{40}$$

On the other hand, the equations of $\alpha_{\boldsymbol{k}}$ and $\beta_{\boldsymbol{k}}$ in our formalism are given by

$$\dot{\alpha}_{\boldsymbol{k}}(t)=\frac{\dot{\Omega}_{\boldsymbol{k}}}{2\Omega_{\boldsymbol{k}}}\beta_{\boldsymbol{k}}\cdot\frac{e^{2i\varphi_\alpha}}{\dot{\Omega}_{\boldsymbol{k}}A_{\boldsymbol{k}}}[2i\dot{\varphi}_\alpha(B_{\boldsymbol{k}}+\Omega_{\boldsymbol{k}})\Omega_{\boldsymbol{k}}+\dot{B}_{\boldsymbol{k}}\Omega_{\boldsymbol{k}}-B_{\boldsymbol{k}}\dot{\Omega}_{\boldsymbol{k}}],$$
$$\dot{\beta}_{\boldsymbol{k}}(t)=\frac{\dot{\Omega}_{\boldsymbol{k}}}{2\Omega_{\boldsymbol{k}}}\alpha_{\boldsymbol{k}}\cdot\frac{e^{-2i\varphi_\alpha}}{\dot{\Omega}_{\boldsymbol{k}}A_{\boldsymbol{k}}^*}[2i\dot{\varphi}_\beta(B_{\boldsymbol{k}}-\Omega_{\boldsymbol{k}})\Omega_{\boldsymbol{k}}+\dot{B}_{\boldsymbol{k}}\Omega_{\boldsymbol{k}}-B_{\boldsymbol{k}}\dot{\Omega}_{\boldsymbol{k}}]. \tag{41}$$

The above two sets of equations are consistent with each other provided that the phases of the coefficients satisfy the transformation rule

$$e^{i\varphi_\alpha}=e^{i\int^t dt'\Omega_{\boldsymbol{k}}(t')}\left(\frac{i\dot{Q}_1+\Omega_{\boldsymbol{k}}Q_1}{-i\dot{Q}_2+\Omega_{\boldsymbol{k}}Q_2}\right)^{1/2},$$
$$e^{i\varphi_\beta}=e^{-i\int^t dt'\Omega_{\boldsymbol{k}}(t')}\left(\frac{-i\dot{Q}_1+\Omega_{\boldsymbol{k}}Q_1}{i\dot{Q}_2+\Omega_{\boldsymbol{k}}Q_2}\right)^{1/2}. \tag{42}$$

Namely, the phase parts, which are undetermined in our present formalism, are chosen in a particular way in the STB formalism. Notice that the right-hand sides of Eqs. (42) are pure phases and hence they are consistent.

IV. SINGLE PARTICLE DISTRIBUTIONS

Let us discuss the qualitative features of the single particle distributions of particles produced to explore the parametric resonance mechanism. The multipion and multisigma state in our mechanism is given by

$$|0\rangle^\sigma\otimes|0\rangle^\pi\equiv|\psi\rangle, \tag{43}$$

where $|0\rangle$ stands for the BCS type squeezed state (39). The factorized form in Eq. (43) stems from the linear approximations described in Sec. II.

The average number of quanta $\langle n\rangle_{\boldsymbol{k}}(t)$ with momentum $\boldsymbol{k}$ at time t is given by

$$\langle n\rangle_{\boldsymbol{k}}(t)=\langle 0|a_{\boldsymbol{k}}^\dagger(t)a_{\boldsymbol{k}}(t)|0\rangle. \tag{44}$$

We suppress in this section the isospin index, since the single particle distributions is independent of isospin. Given the squeezed state (39), it can be readily shown to be

$$\langle n\rangle_{\boldsymbol{k}}(t)=|\beta_{\boldsymbol{k}}|^2=\frac{B_{\boldsymbol{k}}-\Omega_{\boldsymbol{k}}}{2\Omega_{\boldsymbol{k}}} \tag{45}$$

by using Eq. (33) with $B_{\boldsymbol{k}}$ defined in Eq. (28).

Before presenting results of numerical computation, we discuss what would be the characteristic feature of the single particle distributions. It is natural to expect that an enhancement occurs due to the parametric resonance mechanism. With physical values of the parameters, we take the q parameters defined in Eqs. (17) and (18) given by

$$q_\pi=2.0\left(\frac{\chi_0}{v}\right),\quad q_\sigma=6.0\left(\frac{\chi_0}{v}\right). \tag{46}$$

Numerically, q_π and q_σ are less than ~ 0.1 and ~ 0.3, respectively, under the present approximation $(\chi_0/v)<(m_\pi/m_\sigma)^2$. Therefore we are working with narrow resonance approximation. One should keep in mind, however, that the narrow resonance approximation may not hold in the real world.

At such small q parameters, the resonance occurs in the narrow bands at around the discrete values of A, $A=n^2(n=1,2,3,\ldots)$. The first resonance takes place for pion at $A_\pi=1$ and it corresponds to $k=276$ MeV. For sigma, the first resonance takes place at $A_\sigma=4$ at zero momentum. The second resonance would be located at $A_\pi=4$ and at $A_\sigma=9$ which implies that $k=603$ MeV and $k=692$ MeV for pion and sigma, respectively. Since the parameter A is independent of (χ_0/v), we expect that the peak position is stable against varying χ_0, as will be demonstrated below.

We solve the Mathieu equation (23) subject to the boundary condition (35), and then compute $\langle n\rangle_{\boldsymbol{k}}(t)$. In Figs. 1–3 we plot the single particle momentum distributions of pion as a function of momentum $\boldsymbol{k}$ and dimensionless time z with background oscillation parameters $\chi_0/v=0.025$, 0.05, and 0.1. We observe that a prominent peak exists at the right

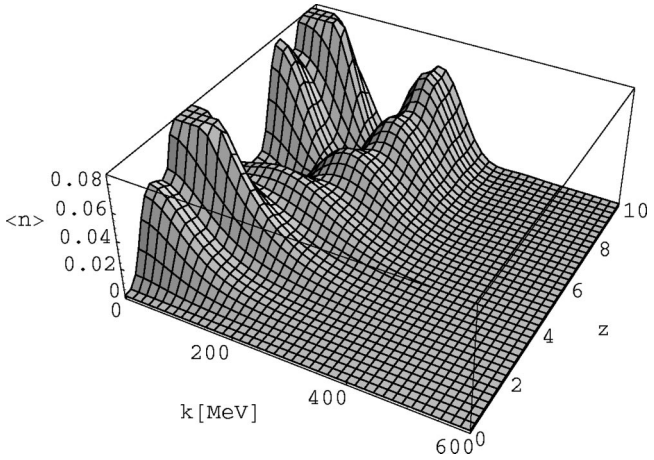

FIG. 1. The single pion momentum distribution as a function of the scaled time $z=\frac{1}{2}(m_\sigma t+\pi)$. The amplitude of oscillation is taken as $\chi_0/v=0.025$.

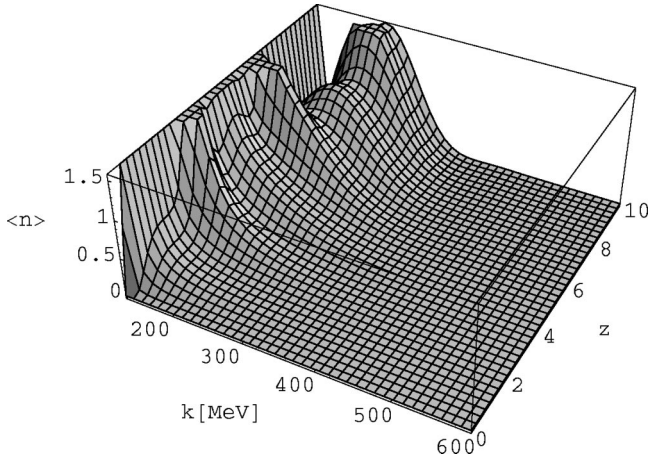

FIG. 3. The single pion momentum distribution as a function of the scaled time $z=\frac{1}{2}(m_\sigma t+\pi)$. The amplitude of oscillation is taken as $\chi_0/v=0.1$.

position for the first resonance in every three figures indicating the parametric resonance enhancement. In Fig. 3 the momentum range $|\boldsymbol{k}|<\sqrt{0.1m_\sigma^2-m_\pi^2}$ in which an exponential instability exists (due to imaginary frequency) and is cut off.

In Fig. 4, we give the single particle momentum distributions of sigma at $\chi_0/v=0.05$. The first resonance, which is expected at $\boldsymbol{k}=0$, is barely seen in the figure. The second resonance is invisible both in pion and sigma distributions.

V. TWO PION CORRELATIONS

We now discuss two particle distributions and correlations between pions. The quantum pion and sigma state is summarized in Eq. (43) under the present approximations. We focus on the pion distributions of various charge states. Because of the factorized form of Eqs. (39) and (43) *n*-particle distributions of σ can readily be obtained from that of π^0 by an appropriate change of the parameters. It is true that the interpretation of our results on sigma particles in real experiments is not very transparent. Furthermore, when the $\sigma\rightarrow\pi\pi$ coupling is turned on the σ particles do affect the two pion correlations. Discussion of this point is, however, beyond the scope of this work.

Two pion distributions are defined as

$$\langle\pi_{\boldsymbol{k}}^i\pi_{\boldsymbol{k}'}^j\rangle\equiv\langle\psi|a_{\boldsymbol{k}}^{i\dagger}(t)a_{\boldsymbol{k}}^i(t)a_{\boldsymbol{k}'}^{j\dagger}(t)a_{\boldsymbol{k}'}^j(t)|\psi\rangle. \tag{47}$$

Because of the factorized form of Eq. (43), there are no correlations between pion and sigma. Also, because of the factorized form of the squeezed state (39) in momentum space, the nontrivial two particle correlations exist only between modes of identical momentum ($\boldsymbol{k}$ and $\boldsymbol{k}$), or between back-to-back momentum ($\boldsymbol{k}$ and $-\boldsymbol{k}$) configurations. One of the most important feature of the state (43) is that it is the isosinglet state. It comes from the fact that the frequency $\Omega_{\boldsymbol{k}}^\pi$ is isospin singlet. As we discuss below, it will give us nontrivial constraints on two pion correlations of various charge combinations. At the same time it also generates the large charge-neutral fluctuations as discussed in Sec. I.

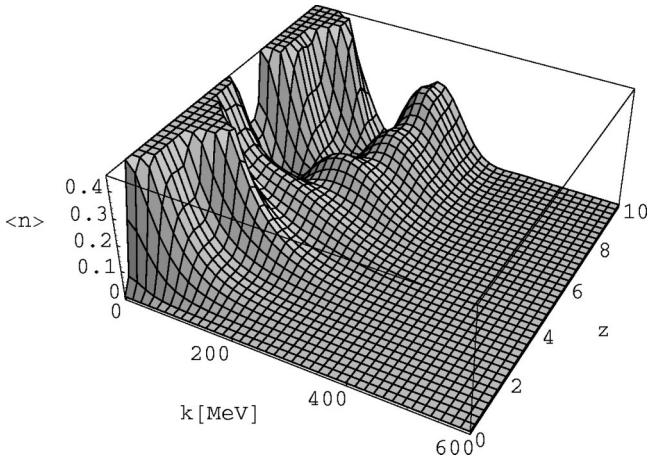

FIG. 2. The single pion momentum distribution as a function of the scaled time $z=\frac{1}{2}(m_\sigma t+\pi)$. The amplitude of oscillation is taken as $\chi_0/v=0.05$.

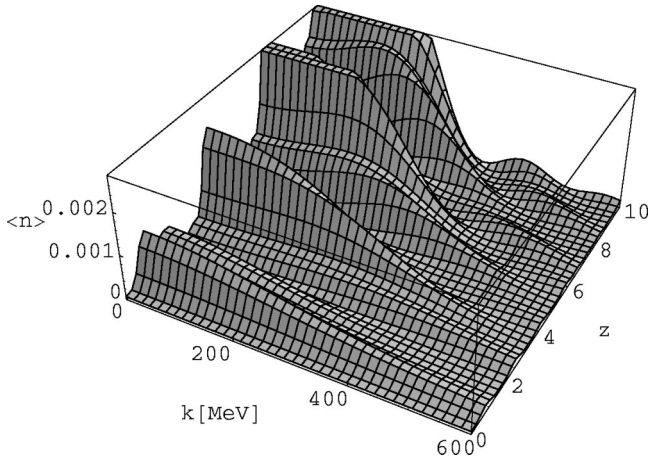

FIG. 4. The single sigma momentum distribution as a function of the scaled time $z=\frac{1}{2}(m_\sigma t+\pi)$. The amplitude of oscillation is taken as $\chi_0/v=0.05$.

In the computation of these quantities, we further recognize that the two pion distributions at zero-momentum *cannot* be obtained by taking the smooth limit $\boldsymbol{k}\to 0$ of the expressions of either identical or back-to-back momentum configurations. It is because $a_{\boldsymbol{k}=0}$ and $a^\dagger_{\boldsymbol{k}=0}$ do not commute, whereas $a_{\boldsymbol{k}}$ and $a^\dagger_{-\boldsymbol{k}}$ do commute for $\boldsymbol{k}\neq 0$. Therefore we have to compute three types of the two-pion distributions separately.

We briefly describe some details of the computation of two pion distributions. It is convenient to use adjoint representation operator $a^i_{\boldsymbol{k}}$ for this purpose. The two pion distribution of the same momentum $\boldsymbol{k}$ goes as follows:

$$\begin{aligned}\langle \pi_{\boldsymbol{k}}\pi_{\boldsymbol{k}}\rangle &= \langle a^\dagger_{\boldsymbol{k}}a_{\boldsymbol{k}}a^\dagger_{\boldsymbol{k}}a_{\boldsymbol{k}}\rangle \\ &= \langle a^\dagger_{\boldsymbol{k}}a^\dagger_{\boldsymbol{k}}a_{\boldsymbol{k}}a_{\boldsymbol{k}}\rangle + \langle a^\dagger_{\boldsymbol{k}}a_{\boldsymbol{k}}\rangle \\ &= \left|\frac{\beta_{\boldsymbol{k}}}{\alpha_{\boldsymbol{k}}}\right|^4 \langle a_{-\boldsymbol{k}}a_{-\boldsymbol{k}}a^\dagger_{-\boldsymbol{k}}a^\dagger_{-\boldsymbol{k}}\rangle + |\beta_{\boldsymbol{k}}|^2 \\ &= \left|\frac{\beta_{\boldsymbol{k}}}{\alpha_{\boldsymbol{k}}}\right|^4 (\langle a^\dagger_{-\boldsymbol{k}}a_{-\boldsymbol{k}}a_{-\boldsymbol{k}}a^\dagger_{-\boldsymbol{k}}\rangle + 2\langle a_{-\boldsymbol{k}}a^\dagger_{-\boldsymbol{k}}\rangle) + |\beta_{\boldsymbol{k}}|^2 \\ &= \left|\frac{\beta_{\boldsymbol{k}}}{\alpha_{\boldsymbol{k}}}\right|^4 (\langle a^\dagger_{-\boldsymbol{k}}a_{-\boldsymbol{k}}a^\dagger_{-\boldsymbol{k}}a_{-\boldsymbol{k}}\rangle + 3\langle a^\dagger_{-\boldsymbol{k}}a_{-\boldsymbol{k}}\rangle + 2) + |\beta_{\boldsymbol{k}}|^2 \\ &= \left|\frac{\beta_{\boldsymbol{k}}}{\alpha_{\boldsymbol{k}}}\right|^4 (\langle \pi_{-\boldsymbol{k}}\pi_{-\boldsymbol{k}}\rangle + 3|\beta_{\boldsymbol{k}}|^2 + 2) + |\beta_{\boldsymbol{k}}|^2, \end{aligned} \tag{48}$$

where the third equality stems from the relation

$$a_{\boldsymbol{k}}|\psi\rangle = \frac{\beta^*_{\boldsymbol{k}}}{\alpha^*_{\boldsymbol{k}}}\cdot a^\dagger_{-\boldsymbol{k}}|\psi\rangle. \tag{49}$$

Similarly, $\langle \pi_{-k}\pi_{-k}\rangle$ is given as

$$\langle \pi_{-\boldsymbol{k}}\pi_{-\boldsymbol{k}}\rangle = \left|\frac{\beta_{\boldsymbol{k}}}{\alpha_{\boldsymbol{k}}}\right|^4 (\langle \pi_{\boldsymbol{k}}\pi_{\boldsymbol{k}}\rangle + 3|\beta_{\boldsymbol{k}}|^2 + 2) + |\beta_{\boldsymbol{k}}|^2. \tag{50}$$

By solving the coupled Eqs. (48) and (50), we obtain two pion distributions of jth isospin component as

$$\langle \pi^j_{\boldsymbol{k}}\pi^j_{\boldsymbol{k}}\rangle = \langle a^\dagger_{\boldsymbol{k}}a_{\boldsymbol{k}}a^\dagger_{\boldsymbol{k}}a_{\boldsymbol{k}}\rangle = |\beta_{\boldsymbol{k}}|^2(2|\beta_{\boldsymbol{k}}|^2+1) = \langle \pi^j_{-\boldsymbol{k}}\pi^j_{-\boldsymbol{k}}\rangle. \tag{51}$$

Via analogous ways, one can compute the following expressions of the elements of nontrivial two pion correlations.

For the same $\boldsymbol{k}\neq 0$:

$$\begin{aligned} &\langle a^\dagger_{i\boldsymbol{k}}a_{i\boldsymbol{k}}\rangle = |\beta_{\boldsymbol{k}}|^2, \\ &\langle a^\dagger_{i\boldsymbol{k}}a_{i\boldsymbol{k}}a^\dagger_{j\boldsymbol{k}}a_{j\boldsymbol{k}}\rangle = |\beta_{\boldsymbol{k}}|^4 \ (\text{for } i\neq j), \\ &\langle a^\dagger_{i\boldsymbol{k}}a_{i\boldsymbol{k}}a^\dagger_{i\boldsymbol{k}}a_{i\boldsymbol{k}}\rangle = |\beta_{\boldsymbol{k}}|^2(2|\beta_{\boldsymbol{k}}|^2+1), \\ &\langle a^\dagger_{i\boldsymbol{k}}a^\dagger_{i\boldsymbol{k}}a_{j\boldsymbol{k}}a_{j\boldsymbol{k}}\rangle = 0 \ (\text{for } i\neq j). \end{aligned} \tag{52}$$

For opposite $\boldsymbol{k}\neq 0$:

$$\begin{aligned} &\langle a^\dagger_{i\boldsymbol{k}}a_{i-\boldsymbol{k}}\rangle = 0, \\ &\langle a^\dagger_{i\boldsymbol{k}}a_{i\boldsymbol{k}}a^\dagger_{j-\boldsymbol{k}}a_{j-\boldsymbol{k}}\rangle = |\beta_{\boldsymbol{k}}|^4 \ (\text{for } i\neq j), \\ &\langle a^\dagger_{i\boldsymbol{k}}a_{i\boldsymbol{k}}a^\dagger_{i-\boldsymbol{k}}a_{i-\boldsymbol{k}}\rangle = |\beta_{\boldsymbol{k}}|^2(2|\beta_{\boldsymbol{k}}|^2+1), \\ &\langle a^\dagger_{i\boldsymbol{k}}a_{j\boldsymbol{k}}a^\dagger_{i-\boldsymbol{k}}a_{j-\boldsymbol{k}}\rangle = |\beta_{\boldsymbol{k}}|^2(|\beta_{\boldsymbol{k}}|^2+1). \end{aligned} \tag{53}$$

By using these formulas, it is straightforward to compute the two pion distributions of definite isospin states. We transform them into the ones written by pion charge states, which are more suitable to gain insights for the experiments. We will describe in Appendix B the relationship between the adjoint representation pion operator (with which we have worked) and the charge-state operator, the (slightly modified) Horn-Silver representation

$$\begin{aligned} a^{(+)}_{\boldsymbol{k}} &= -\frac{1}{\sqrt{2}}(a^1_{\boldsymbol{k}} - ia^2_{\boldsymbol{k}}), \\ a^{(-)}_{\boldsymbol{k}} &= \frac{1}{\sqrt{2}}(a^1_{\boldsymbol{k}} + ia^2_{\boldsymbol{k}}), \\ a^{(0)}_{\boldsymbol{k}} &= a^3_{\boldsymbol{k}}, \end{aligned} \tag{54}$$

where $a^{(\pm)}_{\boldsymbol{k}}$ and $a^{(0)}_{\boldsymbol{k}}$ stand for the annihilation operators of $\pi^\pm$ and π^0 with momentum $\boldsymbol{k}$, respectively. We express the two pion distributions of various charge combinations in the form of the ratio R of them to the single pion distributions as defined by

$$R_{\boldsymbol{k}_1,\boldsymbol{k}_2}(p,q) = \frac{\langle \pi^{(p)}_{\boldsymbol{k}_1}\pi^{(q)}_{\boldsymbol{k}_2}\rangle}{\langle \pi^{(p)}_{\boldsymbol{k}_1}\rangle\langle \pi^{(q)}_{\boldsymbol{k}_2}\rangle}, \tag{55}$$

where p and q stand for $\pm$ and 0. They read (a) identical momentum distribution:

$$\begin{aligned} R_{\boldsymbol{k},\boldsymbol{k}}(+,+) &= R_{\boldsymbol{k},\boldsymbol{k}}(0,0) = 2 + \frac{1}{\langle n\rangle_{\boldsymbol{k}}}, \\ R_{\boldsymbol{k},\boldsymbol{k}}(+,-) &= 1; \end{aligned} \tag{56}$$

(b) back-to-back momentum distribution:

$$\begin{aligned} R_{\boldsymbol{k},-\boldsymbol{k}}(+,-) &= R_{\boldsymbol{k},-\boldsymbol{k}}(0,0) = 2 + \frac{1}{\langle n\rangle_{\boldsymbol{k}}}, \\ R_{\boldsymbol{k},-\boldsymbol{k}}(+,+) &= 1; \end{aligned} \tag{57}$$

(c) zero-momentum distribution:

$$\begin{aligned} R_{\boldsymbol{k}=0,\boldsymbol{k}=0}(+,+) &= R_{\boldsymbol{k}=0,\boldsymbol{k}=0}(+,-) = 2 + \frac{1}{\langle n\rangle_{\boldsymbol{k}=0}}, \\ R_{\boldsymbol{k}=0,\boldsymbol{k}=0}(0,0) &= 3 + \frac{2}{\langle n\rangle_{\boldsymbol{k}=0}}. \end{aligned} \tag{58}$$

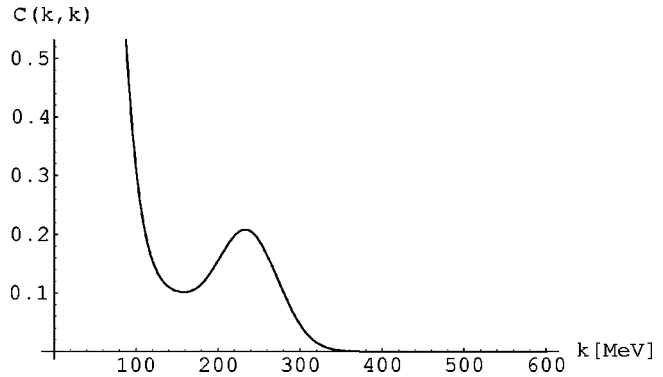

FIG. 5. The pion identical momentum correlation function is depicted. The amplitude of oscillation is taken as $\chi_0/v=0.05$.

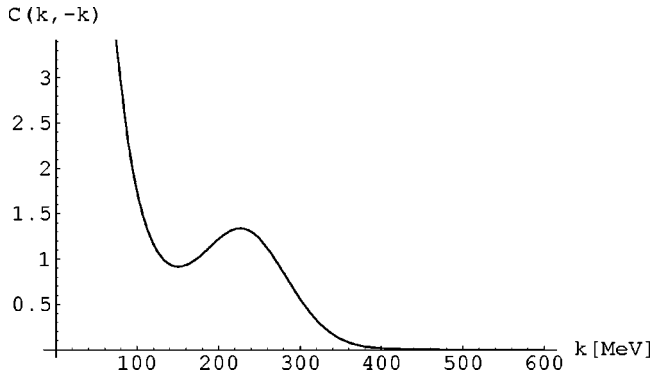

FIG. 6. The pion back-to-back momentum correlation function is depicted. The amplitude of oscillation is taken as $\chi_0/v=0.05$.

As another measure for two pion correlations, we define the correlation function in the following way:

$$C(\pi_{\boldsymbol{k}}^a,\pi_{\boldsymbol{k}'}^b)\equiv\langle\pi_{\boldsymbol{k}}^a,\pi_{\boldsymbol{k}'}^b\rangle-\delta_{ab}\delta_{\boldsymbol{k},\boldsymbol{k}'}\langle\pi_{\boldsymbol{k}}^a\rangle-\langle\pi_{\boldsymbol{k}}^a\rangle\langle\pi_{\boldsymbol{k}'}^b\rangle. \tag{59}$$

Then, it is straightforward to obtain the following results. (a) identical momentum correlations:

$$C(\pi_{\boldsymbol{k}}^+,\pi_{\boldsymbol{k}}^+)=C(\pi_{\boldsymbol{k}}^0,\pi_{\boldsymbol{k}}^0)=\langle n\rangle_{\boldsymbol{k}}^2,$$
$$C(\pi_{\boldsymbol{k}}^+,\pi_{\boldsymbol{k}}^-)=0; \tag{60}$$

(b) back-to-back momentum correlations:

$$C(\pi_{\boldsymbol{k}}^+,\pi_{-\boldsymbol{k}}^-)=C(\pi_{\boldsymbol{k}}^0,\pi_{-\boldsymbol{k}}^0)=\langle n_{\boldsymbol{k}}\rangle(\langle n\rangle_{\boldsymbol{k}}+1),$$
$$C(\pi_{\boldsymbol{k}}^+,\pi_{-\boldsymbol{k}}^+)=0; \tag{61}$$

(c) zero-momentum correlations:

$$C(\pi_{\boldsymbol{k}=0}^+,\pi_{\boldsymbol{k}=0}^+)=\langle n\rangle_{\boldsymbol{k}=0}^2,$$
$$C(\pi_{\boldsymbol{k}=0}^+,\pi_{\boldsymbol{k}=0}^-)=\langle n\rangle_{\boldsymbol{k}=0}(\langle n\rangle_{\boldsymbol{k}=0}+1), \tag{62}$$
$$C(\pi_{\boldsymbol{k}=0}^0,\pi_{\boldsymbol{k}=0}^0)=\langle n\rangle_{\boldsymbol{k}=0}(2\langle n\rangle_{\boldsymbol{k}=0}+1).$$

As will be discussed in Appendix B, the features of the correlation functions in (c) can be understood partly as a consequence of the isospin singlet nature of Eq. (43).

The identical and back-to-back momentum correlations are depicted in Figs. 5 and 6. In these figures, the amplitude parameter is taken as $\chi_0/v=0.05$ and it is integrated over dimensionless time z from 0 to 10, which corresponds to the period of time from $t=0$ to 6.5 fm.

VI. POWER SPECTRUM AND POSSIBLE MECHANISMS FOR AMPLIFICATION OF LOW-MOMENTUM MODES

Now we would like to discuss in some detail the problem of the origin of the long lasting amplification of low-momentum pion modes seen in linear sigma model simulations, in particular in Ref. [4].

Let us first try to make a rough estimate of χ_0/v in their simulation. It is shown in Fig. 2 of Ref. [4] that $\langle\phi^2\rangle$ is given by a constant superposed by an oscillatory component during the time scale of about 10–40 in units of a when large amplification takes place. Here a is the lattice constant and it is taken as $a=(200\ \mathrm{MeV})^{-1}$ in Ref. [4]. Since the frequency of the oscillatory component reflects the pion mass and not the sigma mass it cannot be used to estimate the amplitude of oscillation in the sigma direction. We thus interpret (a quarter of) the constant component as a time and spatially averaged σ oscillation. Since the low-momentum modes are dominant at later times it may be utilized to estimate the amplitude of uniform background σ oscillations in our scheme. Using the constant component of $\sim 0.01a^{-1}$ in $\langle\phi^2\rangle$ we obtain $\chi_0/v\simeq 0.16$. It is a small number and indicates that our approximation is not totally absurd. But it is larger than $(m_\pi/m_\sigma)^2\simeq 0.05$, which implies that the new type of instability mentioned in Sec. III must also be excited.

Since we confine ourselves to $(\chi_0/v)<(m_\pi/m_\sigma)^2$ in this paper, it is not possible to directly compare our parametric resonance mechanism to the Rajagopal-Wilczek simulation. Nevertheless, we attempt to make a bold comparison between these two by estimating the power spectrum, the corresponding quantity to the power calculated by them.

Rajagopal-Wilczek used the definition of power spectrum [25]

$$P_{RW}(\boldsymbol{k},t)=\frac{1}{N^3}\left|\sum_{n_1,n_2,n_3}e^{i\boldsymbol{k}\boldsymbol{n}a}\phi(\boldsymbol{n},t)\right|^2, \tag{63}$$

where N indicates (one-dimensional) box size and they used $N=64$ and $\phi(\boldsymbol{n},t)$ to denote a single component of pion or σ fields at lattice cite $\boldsymbol{n}$. It has the dimension of $(\mathrm{mass})^2$ and hence the ordinates in their Fig. 1 must be understood to be plotted in units of a^{-2}.

We define the corresponding quantity, the power spectrum, in our framework. The natural definition is

$$P_{ours}(\boldsymbol{k},t)=\langle|Q_{\boldsymbol{k}}(t)|^2\rangle. \tag{64}$$

The expectation value $\langle\cdot\rangle$ is to be evaluated by using the normalized squeezed state (39). When the fields are confined

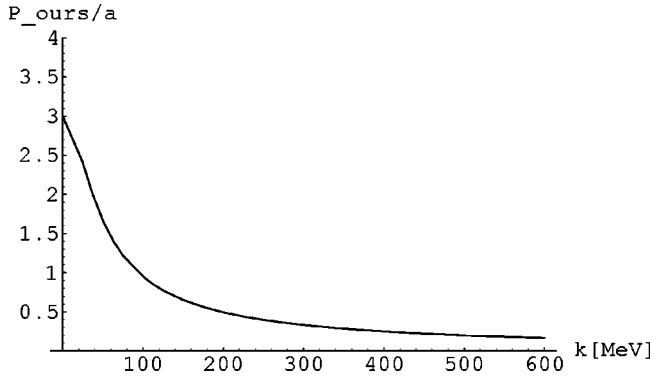

FIG. 7. The power spectrum of pion at $t=0$ is depicted. Due to the boundary condition of no particle production at $t=0$, the power spectrum is not small.

into a finite volume V, the Fourier integral in Eq. (21) is modified to the discrete summation of the form

$$\xi(\boldsymbol{x},t)=\frac{1}{\sqrt{V}}\sum_{k} e^{-i\boldsymbol{k}\boldsymbol{x}}Q_{\boldsymbol{k}}(t), \tag{65}$$

or inversely,

$$Q_{\boldsymbol{k}}(t)=\frac{1}{\sqrt{V}}\int d^3x e^{i\boldsymbol{k}\boldsymbol{x}}\xi(\boldsymbol{x},t). \tag{66}$$

Then, using $V=(\mathrm{Na})^3$, our power spectrum (64) is related with theirs via the following relation:

$$P_{RW}(\boldsymbol{k},t)=P_{ours}(\boldsymbol{k},t)/a^3. \tag{67}$$

It should be noticed that the number presented in Ref. [4] is $P_{RW}(\boldsymbol{k},t)a^2$. Therefore we must plot $P_{ours}(\boldsymbol{k},t)/a$ to compare our power with theirs.

We present our power spectra of pions and sigmas in Figs. 7–10. We have adjusted some parameters so that they accord with the values adopted in Ref. [4]; $v_0=87.4$ MeV, $v=92.5$ MeV, $m_\pi=135$ MeV, though its effect is tiny and

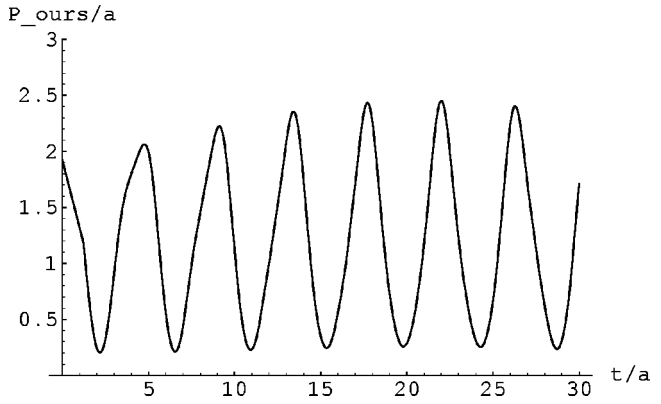

FIG. 8. The time evolution of the power spectrum of pion field at $k=40$ MeV is presented. It corresponds to the longest wavelength bin in Fig. 1 of Rajagopal and Wilczek's paper.

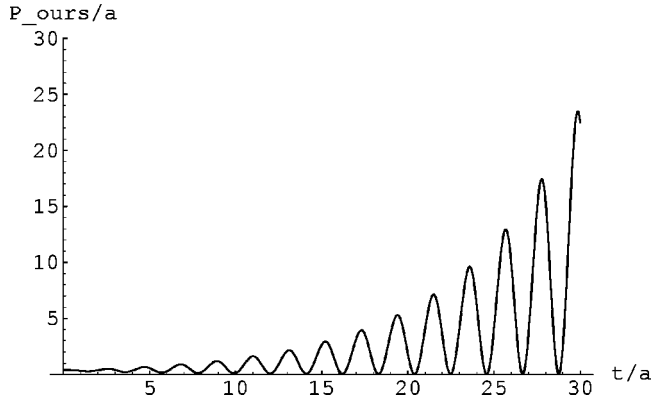

FIG. 9. The time evolution of the power spectrum of pion field at momentum $k=268$ MeV, which corresponds to the first resonance band, is drawn.

does not affect our conclusions. We employ the amplitude parameter of background oscillation as $\chi_0/v=0.05$ in order to avoid the instability.

Plotted in Fig. 7 is the power spectrum of pions at $t=0$. One can see that there is a lot of power at relatively low-momentum modes. One may be curious about the fact that the power is not small at $t=0$ at which we set the boundary condition of no particle production. One can easily verify that it is natural because the latter condition implies that $Q\sim 1/\sqrt{2\Omega}\sim 1/\sqrt{m_\pi}$ and $\dot{Q}\sim\sqrt{\Omega/2}\sim\sqrt{m_\pi}$.

In Fig. 8 we present the time evolution of power of pion field at $k=40$ MeV, which is the longest wavelength case depicted in Fig. 1 in Ref. [4] and is where the largest amplification occurs. We observe that the average power is of order unity as we expect from the above estimation. It is a reasonable result because it is off resonance.

With these parameters, the first resonance appears in $k=268$ MeV and the amplification of the power in this momentum bin is depicted in Fig. 9. The P_{ours}/a is growing by a factor of 50 and reaches to ~ 20 which is a similar order of magnitude with Rajagopal-Wilczek's. Of course, the two numbers cannot be compared directly because of the difference involved between two computations including the initial conditions. Nevertheless, the qualitative feature of the growing power to the same order of magnitude may be an

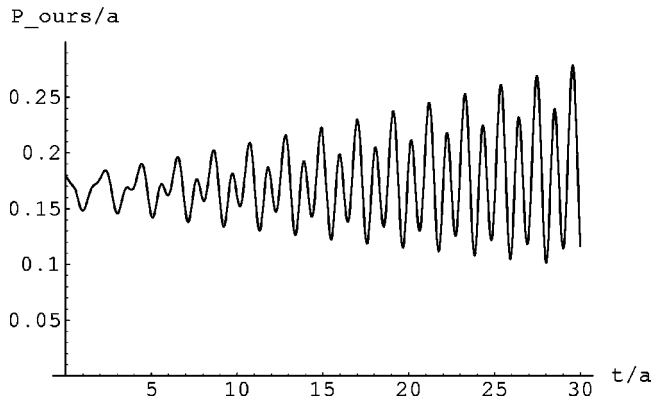

FIG. 10. The time evolution of the power spectrum of sigma field at $k=40$ MeV is depicted.

indication that the parametric resonance mechanism plays an important role in the long lasting amplification of low-momentum modes. One may argue that our results and those of Rajagopal-Wilczek are qualitatively different because the amplification occurs in low momentum modes in their simulation, whereas it happens at resonance in our case. However, if we had not ignored the nonlinearity it might have mediated the enhancement at resonance to other modes.

Plotted in Fig. 10 is the time evolution of the power of sigma field at $k=40$ MeV as in Fig. 8. The power of sigmas is an order of magnitude smaller than that of pions, in agreement with the feature obtained in Rajagopal-Wilczek's simulation.

We now summarize our present understanding on the possible origin of the long lasting amplification of low-momentum pion modes seen in the linear sigma model simulations. We have suggested that the parametric resonance might be the cause. The semiquantitative features of the power spectrum including its order of magnitude and the rate of growth is not inconsistent with our proposal. We also pointed out that a new type of instability exists in our approximation scheme which, if real, would enhance the amplification of low-momentum modes. We, however, failed to achieve an intuitive understanding of the physical origin of the new instability.

VII. CONCLUSION AND DISCUSSION

We have discussed the pion production via the parametric resonance mechanism within the linear sigma model. In particular, stimulated by the feature of the numerical simulations of the linear sigma model, we focused on the scenario in which classical background oscillations of the sigma model fields are in the σ direction. Assuming small amplitude oscillation which may be natural in the late stage of evolution of DCC, we have shown that one can ignore effects due to nonlinearity and quantum back reactions for a sufficiently long time. Thanks to this fact, we were able to construct an explicit quantum pion (and sigma) state which allows us to calculate the two particle correlations as well as the single particle distributions.

Our treatment, though under very restrictive assumptions, may be good enough to illuminate characteristic features of the parametric resonance mechanism. We formulated the quantum theory of the system with Mathieu instability on a more conventional basis of quantum field theory and clarified the relationship between our formalism and the one given by Shtanov, Traschen, and Brandenberger [17].

We have analyzed the computed single particle distributions and clarified the structure of narrow resonances characteristic to the parametric resonance mechanism. We then discussed the two pion correlations as a possible experimental probe for disoriented chiral condensate. Since the two pion correlations have unique characteristics, the back-to-back (in momentum space) correlations, it must give a clear signature which should merit the experimental hunting of DCC. In particular, it cannot be masked by the identical particle interference, the Hanbury Brown–Twiss effect [26].

Why two particle correlation? It is certainly far more difficult to measure compared with the multiplicity distributions, on which all the recent experimental searches for DCC rely [27,28]. The global analysis using multiplicity distributions is powerful if large fractions of events are accompanied by the DCC domain formation. On the other hand, a different strategy is required for hunting if DCC is a rare phenomenon.

We have discussed possible origin of the long lasting amplification of low-momentum pion modes in the last section. Our discussion cannot be a complete one, but we hope that it stimulates the readers' interests in this problem.

We should mention the limitation and the drawback in our treatment in this paper. We ignored the quantum back reaction and the instability of σ meson which should exist in the real world. It is a perfectly legitimate approximation if the amplitudes of background σ oscillations are really small. However, it is possible that the amplitudes are sometimes large because of the prevailing thermal fluctuations in the initial stage. Since we are dealing with the system in which the coupling is really strong, most probably, the peak in the single particle distributions will go away after the quantum back reaction is taken into account.

Then, the key question is whether anything in our results remains valid after the quantum back reaction is taken into account. We argue that the answer is yes; it is the characteristic features of the two pion correlations which are discussed in detail in Sec. V. We are now engaged in a computation to verify our expectation.

What about the $\sigma \rightarrow \pi\pi$ coupling? It is clear that it also tends to smear out the resonance peaks and, more importantly, may obscure the signature of the back-to-back correlations. Again we need a more elaborate treatment which includes the instability of σ to make a definitive statement about how much the signature survives in the case with $\sigma \rightarrow \pi\pi$ coupling. The formalisms which may be suitable for such analysis have been investigated in detail [29,30].

There are also some recent proposals [31,32] that the hadronic medium effects may induce the similar back-to-back correlations in momentum space, which would mimic the signature of DCC discussed in this paper. One would hope that it should be possible to find observational features which discriminate these two mechanisms. The task is, however, beyond the scope of this paper.

ACKNOWLEDGMENTS

During the long-term investigation we benefited from numerous conversations in various stages of this work with Masayuki Asakawa, Dan Boyanovsky, Berndt Müller, Krishna Rajagopal, and Valery Rubakov. In particular we thank Krishna Rajagopal for his informative and kind correspondences in comparing power spectra obtained by our calculation and their calculation. The research of H.M. was partly supported by the Grant-in-Aid for International Scientific Research No. 09045036, Inter-University Cooperative Research, and the Grant-in-Aid for Scientific Research in Priority Areas No. 11127213, Ministry of Education, Science, Sports and Culture of Japan.

APPENDIX A

We discuss in this appendix some aspects of multiparticle correlations among particles involved in a normalized single-mode squeezed state,

$$|\psi\rangle = \frac{1}{\sqrt{\langle 0|e^{\gamma^* K_-} e^{\gamma K_+}|0\rangle}}\, e^{\gamma K_+}|0\rangle, \tag{A1}$$

where $K_+ = \frac{1}{2}(a^\dagger)^2$ and $K_- = \frac{1}{2}(a)^2$, and γ denotes a complex number. The operators K_+ and K_-, together with $N = a^\dagger a$, form a closed algebra,

$$[K_-, K_+] = N + \frac{1}{2}, \quad [N, K_\pm] = \pm 2K_\pm, \tag{A2}$$

which will play a role in our following computation.

For convenience in the systematic treatment, we employ the generating function formalism developed by Koba, Nielson, and Olesen [33] and by Koba [34]. The generating function is defined by

$$F[h] = \sum_{n=0}^{\infty} (1+h)^n P_n, \tag{A3}$$

using the multiplicity distribution $P_n = |\langle n|\psi\rangle|^2$ where

$$|n\rangle = \frac{(a^\dagger)^n}{\sqrt{n!}}\,|0\rangle. \tag{A4}$$

The generating function can generate a whole set of various moments when expanded in various manners:

$$F[h] = \sum_{n=0}^{\infty} \frac{h^k}{k!} F^{(k)} = \exp\left[\sum_{k=0}^{\infty} \frac{h^k}{k!} C^{(k)}\right]. \tag{A5}$$

In these equations, $F(k)$ denotes

$$F^{(k)} = \langle n(n-1)(n-2)\cdots(n-k+1)\rangle, \tag{A6}$$

where $\langle\cdots\rangle$ implies the average over by the multiplicity distribution P_n; $\langle O\rangle \equiv \Sigma_{n=0}^{\infty} O_n P_n$. As is familiar in cluster expansion in statistical mechanics, $C^{(k)}$ represents the correlations

$$\begin{aligned} C^{(1)} &= \langle n\rangle, \\ C^{(2)} &= \langle n(n-1)\rangle - \langle n\rangle^2, \\ C^{(3)} &= \langle n(n-1)(n-2)\rangle - 3\langle n(n-1)\rangle\langle n\rangle - \langle n\rangle^3, \end{aligned} \tag{A7}$$

and so on.

The expression of the generating function in a form of operator expectation value is give by Koba [34]:

$$F[h] = \langle\psi| :e^{ha^\dagger a}: |\psi\rangle, \tag{A8}$$

where :: indicates to take the normal ordering. It proves to be a very useful formula for our purpose. Toward calculating $F[h]$, we define the quantity A_m as $A_m \equiv \langle\psi|(a^\dagger)^m (a)^m|\psi\rangle$. Using the algebra applied to the vacuum state

$$\begin{aligned} [a^m, e^{\gamma K_+}]|0\rangle &= \gamma a^{m-1} a^\dagger e^{\gamma K_+}|0\rangle, \\ \langle 0|[e^{\gamma^* K_-}, (a^+)^m] &= \gamma^* \langle 0|e^{\gamma^* K_-} a (a^\dagger)^{m-1}, \end{aligned} \tag{A9}$$

one can derive the recursion relation among A_m,

$$\begin{aligned} A_0 &= 1, \\ A_1 &= \langle n\rangle, \\ A_{m+2} &= \langle n\rangle[(2m+3)A_{m+1} + (m+1)^2 A_m] \quad (m \geqslant 0). \end{aligned} \tag{A10}$$

One can show, by direct computation, that

$$\langle n\rangle = \langle\psi|a^\dagger a|\psi\rangle = \frac{|\gamma|^2}{1-|\gamma|^2}. \tag{A11}$$

We can convert the recursion relation (A10) into the differential equation obeyed by the generating function

$$\left[\left(h^2 + 2h - \frac{1}{\langle n\rangle}\right)\frac{d^2}{dh^2} + 3(h+1)\frac{d}{dh} + 1\right] F[h] = 0. \tag{A12}$$

We make a change of variable

$$t = \frac{\langle n\rangle}{1+\langle n\rangle}(1+h)^2 \tag{A13}$$

to transform the differential equation into the standard form

$$\left[t(1-t)\frac{d^2}{dt^2} + \left(\frac{1}{2} - 2t\right)\frac{d}{dt} - \frac{1}{4}\right] F[t] = 0. \tag{A14}$$

The solution to the equation subject to the boundary conditions

$$\begin{aligned} F[t]|_{t=\langle n\rangle/(1+\langle n\rangle)} &= 1, \\ F'[t]|_{t=\langle n\rangle/(1+\langle n\rangle)} &= \frac{1+\langle n\rangle}{2}, \end{aligned} \tag{A15}$$

is uniquely given by

$$F[t] = \frac{1}{\sqrt{(1+\langle n\rangle)(1-t)}}. \tag{A16}$$

The boundary conditions correspond to $A_0 = 1$, $A_1 = \langle n\rangle$, and $A_2 = \langle n\rangle(3\langle n\rangle + 1)$. Thus we have obtained the generating function as

$$F[h] = \frac{1}{\sqrt{1 - \langle n\rangle(h^2+2h)}}. \tag{A17}$$

The correlation moments can be easily computed as follows:

$$C^{(1)}=\langle n\rangle,$$

$$C^{(2)}=\langle n\rangle(2\langle n\rangle+1),$$

$$C^{(3)}=2\langle n\rangle^2(4\langle n\rangle+1), \tag{A18}$$

$$C^{(4)}=48\langle n\rangle^2\left(\langle n\rangle^2+\langle n\rangle+\frac{1}{8}\right).$$

Since the generating function (A17) is the function of $(1+h)^2$, the multiplicity distribution P_n for odd n vanishes. That for even n is given by

$$P_{2k}=\frac{(2k)!}{2^{2k}(k!)^2}\frac{1}{\sqrt{1+\langle n\rangle}}\left(\frac{\langle n\rangle}{1+\langle n\rangle}\right)^k, \tag{A19}$$

which is nothing but the negative binomial distribution familiar in hadronic multiparticle phenomenology. The expression (A19) reproduces the results obtained by Yoshimura [23] who also calculated all the off-diagonal elements of the density matrix.

For completeness, we calculate the Koba-Nielsen-Olesen (KNO) scaling function for the multiplicity distribution (A19). It is obvious, from the expression of the correlation moments, that the squeezed state has ''long range'' correlations

$$\frac{C^k}{\langle n\rangle^k}\xrightarrow[\langle n\rangle\to\infty]{}\text{finite}. \tag{A20}$$

The multiplicity distribution obeys the KNO scaling behavior. Either by solving the moment problem or by using the explicit form (A19), one can show that

$$\psi(z)=\lim_{\langle n\rangle\to\infty}\langle n\rangle P_n=\sqrt{\frac{2}{\pi z}}e^{-z/2}. \tag{A21}$$

APPENDIX B

We derive relations among two pion correlation functions of various charge states which follow from isospin invariance. We restrict ourselves to the case with isosinglet state which is of concern to us. We also confine ourselves to the case of zero momentum pions; the treatment for nonzero momentum pions is different and is much more involved.

We work with the (slightly modified) Horn-Silver [35] representation of the isospin generator

$$\vec{T}=a^{i\dagger}\vec{\tau}_{ij}a^j \quad (i,j=+,-,0), \tag{B1}$$

where

$$\tau_1=\frac{1}{\sqrt{2}}\begin{bmatrix}0&0&1\\0&0&1\\1&1&0\end{bmatrix},\quad \tau_2=\frac{1}{\sqrt{2}}\begin{bmatrix}0&0&-i\\0&0&i\\i&-i&0\end{bmatrix},$$

$$\tau_2=\begin{bmatrix}1&0&0\\0&-1&0\\0&0&0\end{bmatrix}. \tag{B2}$$

The explicit form of $\vec{T}$ is as follows:

$$T^1=\frac{1}{\sqrt{2}}[a^{(+)\dagger}a^{(0)}+a^{(0)\dagger}(a^{(+)}+a^{(-)})+a^{(-)\dagger}a^{(0)}],$$

$$T^2=\frac{i}{\sqrt{2}}[-a^{(+)\dagger}a^{(0)}+a^{(0)\dagger}(a^{(+)}-a^{(-)})+a^{(-)\dagger}a^{(0)}], \tag{B3}$$

$$T^3=\frac{1}{\sqrt{2}}[a^{(+)\dagger}a^{(+)}-a^{(-)\dagger}a^{(-)}],$$

where $a^{(+)}$, $a^{(0)}$, and $a^{(-)}$ are the annihilation operators of π^+, π^0, and π^-, respectively, as defined in Eq. (54). The relation between the charge eigenstate operators and the adjoint representation operators are given in Eq. (54).

Let $|\psi\rangle$ be the isosinglet state. Then, it is annihilated by the isospin operator, $\vec{T}|\psi\rangle=0$. From this, it follows that

$$\langle\psi|e^{i\vec{\xi}\cdot\vec{T}}a^{k\dagger}a^l|\psi\rangle=\langle\psi|a^{k\dagger}a^l|\psi\rangle \tag{B4}$$

for any k,l. This is the relation that should be obeyed for all orders in $\vec{\xi}$. If we take the first-order term in $\vec{\xi}$, we obtain the sum rule

$$\langle\psi|\vec{T}a^{k\dagger}a^l|\psi\rangle=0 \quad (\text{for any } k,l). \tag{B5}$$

Due to isospin invariance, it is easy to show that $\langle\pi^+\rangle=\langle\pi^-\rangle=\langle\pi^0\rangle$. Then, the T^1 (or T^2) sum rule produces relations like

$$\langle\pi^+\pi^0\rangle=\langle\pi^-\pi^0\rangle, \tag{B6}$$

which also follows from the T^3-sum rule. The useful relations comes from the T^3-sum rule

$$\langle\pi^+\pi^+\rangle=\langle\pi^+\pi^-\rangle=\langle\pi^-\pi^-\rangle. \tag{B7}$$

In these equations, $\langle\pi^\alpha\pi^\beta\rangle$ implies the two pion distribution of charge state α and β.

The two pion correlation function may be defined as

$$C(\pi^+,\pi^+)=\langle\pi^+\pi^+\rangle-\langle\pi^+\rangle-\langle\pi^+\rangle^2,$$

$$C(\pi^+,\pi^0)=\langle\pi^+\pi^0\rangle-\langle\pi^+\rangle\langle\pi^0\rangle, \tag{B8}$$

etc. Then, we obtain the isospin sum rule

$$C(\pi^+,\pi^-)=C(\pi^+,\pi^+)+\langle\pi\rangle, \tag{B9}$$

where $\langle\pi\rangle\equiv\langle\pi^+\rangle=\langle\pi^-\rangle=\langle\pi^0\rangle$. Since $\langle\pi\rangle$ is positive, the inequality among two pion correlations follows:

$$C(\pi^+,\pi^-)>C(\pi^+,\pi^+). \tag{B10}$$

It may be surprising that the unlike-sign correlation is stronger than the like-sign correlation; this is a consequence of the isospin invariance with isosinglet nature of the multipion state.

[1] Y. Fujimoto, C. M. G. Lattes, and S. Hasegawa, Phys. Rep. **65**, 151 (1980); L. T. Baradzei *et al.*, Nucl. Phys. **B370**, 365 (1992); J. Lord and J. Iwai (unpublished).

[2] Early discussions on DCC may be found, e.g., in A. A. Anselm, Phys. Lett. B **217**, 169 (1989); A. A. Anselm and M. G. Ryskin, *ibid.* **266**, 482 (1991); J.-P. Blaizot and A. Krzywicki, Phys. Rev. D **46**, 246 (1992); **50**, 442 (1994).

[3] J. D. Bjorken, Acta Phys. Pol. B **23**, 561 (1992); J. D. Bjorken, *ibid.* **28**, 2773 (1997); J. D. Bjorken, K. L. Kowalski, and C. C. Taylor, talk at 7th Rencontres de Physique de laValee d'Aoste, La Thuile Rencontres 1993, p. 507 (unpublished).

[4] K. Rajagopal and F. Wilczek, Nucl. Phys. **B404**, 577 (1993); K. Rajagopal, in *QCD Phase Transitions*, edited by H. Feidmeier, J. Knoll, W. Norenberg, and J. Wambach (GSI, Darmstadt, 1997), p. 458.

[5] M. Asakawa, Z. Huang, and X.-N. Wang, Phys. Rev. Lett. **74**, 3126 (1995).

[6] C. Greiner, C. Gong, and B. Müller, Phys. Lett. B **316**, 226 (1993).

[7] K. Rajagopal and F. Wilczek, Nucl. Phys. **B399**, 395 (1993).

[8] L. D. Landau and E. M. Lifshiz, *Mechanics* (Pergamon Press, New York, 1960) p. 80.

[9] S. Mrówczyński and B. Müller, Phys. Lett. B **363**, 1 (1995).

[10] J. Randrup, Phys. Rev. Lett. **77**, 1226 (1996); J. Randrup and R. L. Thews, Phys. Rev. D **56**, 4392 (1997).

[11] H. Minakata and B. Müller, Phys. Lett. B **377**, 135 (1996); M. Asakawa, H. Minakata, and B. Müller, Phys. Rev. D **58**, 094011 (1998); **A638**, 443c (1998).

[12] D. Boyanovsky, H. J. de Vega, R. Holman, and S. P. Kumar, Phys. Rev. D **56**, 3929 (1997); S. P. Kumar, D. Boyanovsky, H. J. de Vega, and R. Holman, hep-ph/9905374.

[13] D. I. Kayser, Phys. Rev. D **59**, 117901 (1999).

[14] For an attempt to model the mediation mechanism, see H. Minakata, Nonequilibrium Aspects of DCC's, talk at RIKEN BNL Research Center Workshop on ''Quantum Fields In & Out of Equilibrium,'' 1998, Brookhaven National Laboratory, Upton, New York.

[15] H. Hiro-Oka and H. Minakata, Phys. Lett. B **425**, 129 (1998); **434**, 461 (1998).

[16] M. Abramowitz and I. A. Stegun, *Handbook of Mathematical Functions* (Dover, New York, 1965).

[17] Y. Shtanov, J. Traschen, and R. Brandenberger, Phys. Rev. D **51**, 5438 (1995).

[18] H. P. Yuen, Phys. Rev. A **13**, 2226 (1976); D. F. Walls, Nature (London) **306**, 141 (1983); D. F. Smirnov and A. S. Troshin, Usp. Fiz. Nauk **153**, 233 (1987) [Sov. Phys. Usp. **30**, 851 (1987)].

[19] I. I. Kogan, Pis'ma Zh. Éksp. Teor. Fiz. **59**, 332 (1994) [JETP Lett. **59**, 312 (1994)]; R. D. Amado and I. I. Kogan, Phys. Rev. D **51**, 190 (1995).

[20] I. M. Dremin and R. C. Hwa, Phys. Rev. D **53**, 1216 (1996).

[21] L. Kofman, A. Linde, and A. A. Starobinsky, Phys. Rev. Lett. **73**, 3195 (1994); Phys. Rev. D **56**, 3258 (1997).

[22] D. Boyanovsky, H. J. de Vega, R. Holman, D.- S. Lee, and A. Singh, Phys. Rev. D **51**, 4419 (1995); D. Boyanovsky, H. J. de Vega, R. Holman, and J. F. J. Salgado, *ibid.* **54**, 7570 (1996).

[23] M. Yoshimura, Prog. Theor. Phys. **94**, 873 (1995); H. Fujisaki, K. Kumekawa, M. Yamaguchi, and M. Yoshimura, Phys. Rev. D **53**, 6805 (1996); **54**, 2494 (1996).

[24] D. J. H. Chung, E. W. Kolb, and A. Riotto, Phys. Rev. Lett. **81**, 4048 (1998); Phys. Rev. D **59**, 023501 (1999); V. Kuzmin and I. Tkachev, Pis'ma Zh. Éksp. Teor. Fiz. **68**, 255 (1998) [JETP Lett. **68**, 271 (1998)]; M. Arai, H. Hiro-Oka, N. Okada, and S. Sasaki, Phys. Lett. B **449**, 230 (1999).

[25] K. Rajagopal, in *Quark-Gluon Plasma 2*, edited by R. C. Hwa (World Scientific, Singapore, 1995), p. 484.

[26] R. Hanbury-Brown and R. Q. Twiss, Philos. Mag. **45**, 633 (1954); G. Goldhaber, S. Goldhaber, W. Lee, and A. Pais, Phys. Rev. **120**, 300 (1960); E. V. Shuryak, Phys. Lett. B **44**, 387 (1973); Yad. Fiz. **18**, 1302 (1974) [Sov. J. Nucl. Phys. **18**, 667 (1974)]; G. I. Kopylov and M. I. Podgoretsky, *ibid.* **14**, 1081 (1971); [**14**, 604 (1972)]; G. I. Kopylov, Phys. Lett. **50B**, 472 (1974).

[27] MiniMax Collaboration, T. Brooks *et al.*, Phys. Rev. D **55**, 5667 (1997); J. Street (unpublished).

[28] WA98 Collaboration, M. M. Aggarwal *et al.*, Phys. Lett. B **420**, 169 (1998); Nucl. Phys. **A638**, 249c (1998).

[29] D. Boyanovsky, H. J. de Vega, and R. Holman, Phys. Rev. D **51**, 734 (1995); D. Boyanovsky, H. J. de Vega, R. Holman, D.-S. Lee, and A. Singh, *ibid.* **51**, 4419 (1995).

[30] F. Cooper, Y. Kluger, E. Mottola, and J. E. Paz, Phys. Rev. D **51**, 2377 (1995); F. Cooper, S. Habib, Y. Kluger, and E. Mottola, *ibid.* **55**, 6471 (1997).

[31] M. Asakawa and T. Csörgö, Heavy Ion Phys. **4**, 233 (1996); M. Asakawa, T. Csörgö, and M. Gyulassy, Phys. Rev. Lett. **83**, 4013 (1999); T. Csörgö and M. Gyulassy, in *Proceedings of Correlations and Fluctuations '98*, edited by T. Csorgo, S. Hegyi, G. Jansco, and R. C. Hwa (World Scientific, Singapore, 1999), p. 547.

[32] I. L. Andreev, Mod. Phys. Lett. A **14**, 459 (1999).

[33] Z. Koba, H. B. Nielsen, and P. Olesen, Nucl. Phys. **B40**, 317 (1972).

[34] Z. Koba (unpublished).

[35] D. Horn and R. Silver, Ann. Phys. (Paris) **66**, 509 (1971).